Jour.Korean Inst. Mining Geol.
Vol. 24, No.4, p.447-463,1991.

Geochemistry of Precambrian Mafic Dikes in Northern Michigan, U.S.A.: Implications for the Paleo-Tectonic Environment

Soo Meen Wee*

ABSTRACT : Petrological and chemical studies of Precambrian dikes in the southern Lake Superior region were conducted with the objects of evaluating magma source and constraining models for the paleo-tectonic environment. Forty-six samples were analyzed for major, trace, and rare earth elements. Chemical data of the studied dikes are typical of continental tholeiites and showing iron-enrichment fractionation trend. With wallrock contamination carefully evaluated, a series of tectonic discriminating methods utilizing immobile trace elements indicate that the source magma was a high-Ti tholeiitic basalt similar to present-day T-type MORB. Effect of chemical contamination from wallrock assimilation accmulates with increasing differentiation. Evolved rocks show LREE enriched patterns and have enhanced levels of LIL elements (e.g., Rb, K, Ba, Th), but low levels of high field strength elements (e.g., Nb, P, Ti) with respect to their neighboring elements. It is suggested from this study that this enrichment possibly due to a combination of a feature inherited from the subcontinental lithosphere and crustal contamination. Geochemical signatures of these rocks are distinctively different from those of arc-related volcanics. Comparisons with chemistries of modern magmas show a pattern of overlap between Within-plate and ocean-floor characteristics, and chemical signatures of these rocks favor a model of intrusion into a crustal environment undergoing lithospheric attenuation.

INTRODUCTION

Dike swarms of Proterozoic age are of widespread occurrence in many Precambrian cratons such as Scourie dikes in Scotland, Abitibi and Sudbury swarms in southern Canadian Shield, Keweenawan dike swarm in northern Michigan, and Mackenzie dike swarm, fans southwards from the Arctic coast near Coronation Gulf, to northwestern Ontario. In southern Lake Superior region, Archean and Proterozoic dikes ranging in age from 2.6 to 1.0 Ga form at least three swarms that differ from one another in trend, mineralogy, and composition. This investigation is focused on the early Proterozoic metadiabasic dikes. The dike swarm may be many tens of kilometers broad and individual dikes may extend for well over 10 km. Emplacement of the dike swarms may be related to major tectonic events, including rifting and continental collision, that have affected this part of the Precambrian craton.

Previous studies of the dike swarms are few and could not be used to evaluate petrochemical variations within the swarms either temporally and spatially, or may they be used to allow meaningful comparisons to rocks from modern, known tectonic environments. Thus, more data must be obtained before reasonable petrogenetic/tectonic interpretations can be made for this stage of development of the North America craton. Such a knowledge of petrogenetic history will provide constraints on the tectonic evolution of the study area.

The main objectives of this research were to characterize magmas associated with a proposed early Proterozoic plate margin and to examine the nature of plate tectonics in the Lake Superior region. Precambrian dikes from northern Michigan were sampled and analyzed for major, trace and rare earth elements to evaluate the mantle source composition and extent of fractional crystallization of the magmas. Chemical characteristic patterns of immobile elements, diagnostic of tectonic setting in modern magmas, were applied to these rocks in an attempt to determine their environment of emplacement.

GENERAL GEOLOGY

Regional Overview

The Lake Superior region marked the southern extend of the North Amerca craton during the Proterozoic. Early Proterozoic strata in the Lake Superior region show evidence for a

* Center for Mineral Resources Research Anamdong 5ga, Sungbuk-ku, Seoul, Korea.

complex tectonic history. The area has been involved in two major orogenic episodes, the Algoman Orogeny (2.7 Ga) and the Penokean Orogeny, which occurred about 1.85-1.9 Ga ago and included deformation, regional metamorphism, and extrusive and intrusive igneous activities (Cannon, 1973; Van Schmus, 1976).

The area was divided into four tectono-stratigraphic terranes by Larue (1983). The terranes are 1) the passive margin terrane, 2) the Crystal Falls terrane, 3) the Florence-Niagara terrane, and 4) the northern Wisconsin magmatic arc terrane (Fig. 1).

The passive margin terrane is composed of three transgressive metasedimentary sequences deposited unconformably on Archean sialic crust. The metasedimentary sequence, from the oldest to youngest, are the Chocolay, the Menominee and the Baraga Groups.The Chocolay Group has characteristics in common with a modern miogeosynclinal or shelf sea facies association (Cambray, 1978). The tectonic conditions were apparently relatively stable during the deposition of Chocolay Group strata.

The Menominee Group is a fining upward sequence with a basal quartzite overlain by laminated argillites, and chemical precipitates with local conglomerates (Klasner and Cannon, 1978). It was deposited unconformably on the lower Precambrian basement rocks with mild tectonic disturbances during sedimentation (Van Schmus, 1976; Cambray, 1978). Rapid subsidence of the area resulted in a deep water environment. An extensive period of erosion seems to have occurred before the first formation of Baraga Group was laid down (Cambray, 1978).

The Baraga Group is composed of a basal quartzite, a iron formation, and the tholeiitic basalts of the Hemlock Formation, followed by deposition of turbidites of the Michigamme Slate (James et al., 1968; Larue and Sloss, 1980). The composition of these volcanic rocks change from felsic in the northeast to mafic to the southwest (Cannon and Klasner, 1976). Basaltic dikes were intruded into the adjacent Archean rocks, and sills were intruded into the passive margin sediments. These dikes, the subject of this study, were emplaced in the Baraga

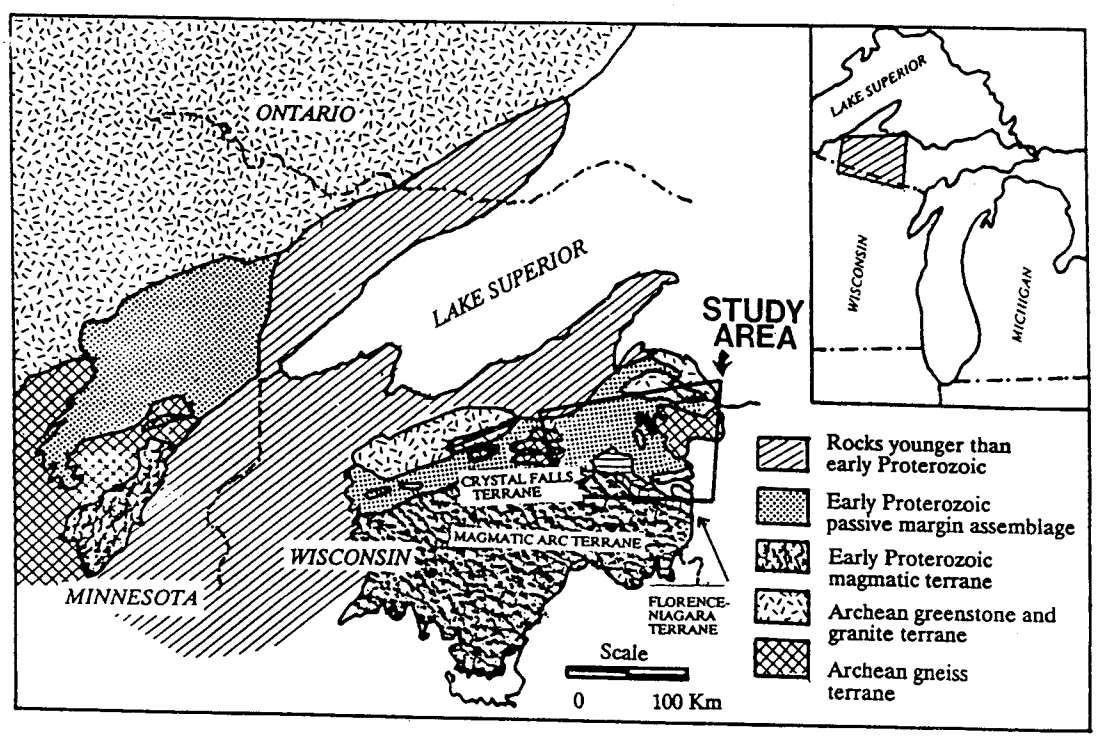

Fig. 1. .Early Proterozoic tectonostratigraphic terranes in the southern Lake Superior region.

group as an equivalent to the basaltic extrusives (Cannon, 1973). Although the exact relative age of any individual dike is indeterminate, some dikes, if not most, have been interpreted as predating the Penokean Orogeny (Cannon, 1975; Baxter and Bornhorst, 1988).

The Crystal Falls terrane is composed of the Paint River Group and the underlying Badwater greenstones, a thick units of pillow basalts and greenstones (James et al., 1968). The contact of Paint River Group with the underlying Badwater greenstone has been inferred to be a fault along the northern border of the Crystal Falls terrane (Larue, 1983), or an unconformity (James et al., 1968). The Paint River Group, a sequence of deposits derived in part from terrigeneous sources, may be equivalent to the Menominee Group (Cambray, 1978), however, others believe the Paint River Group to be separated from the Menominee Group by the Baraga Group (James, 1958; Cannon and Gair, 1970).

The Florence-Niagara terrane consists of eight major fault-bounded packets that strike E-W to NW-SE (Larue and Ueng, 1988). The fault-bounded packets containing highly deformed rocks that are, for the most part, correlative with the passive margin terrane (Larue, 1983).

The magmatic arc terrane consists of several cores of granitoid to gneissic rocks mantled by highly deformed metavolcanic, metapellitic, and metagabbroic rocks. This area shows a record that records a major interval of calc-alkaline and tholeiitic volcanism at 1.86-1.87 Ga (Sims, 1988). Granitoid intrusions, which compose about one-quarter of the exposed part of the magmatic arc terrane, accompanied and followed the volcanism. The metavolcanic rocks bear geochemical signatures typical of volcanic arc environments (Van Schmus, 1976; Cudzilo, 1978; Greenberg and Brown, 1983; Ueng et al., 1988).

Tectonic Models

Several tectonic models have been proposed for the Lake Superior region in early Proterozoic time. Morey and Sims (Morey, 1978; Sims, 1976) suggested that the metavolcanic sediments were deposited and deformed in a large intracratonic basin and that two types of Archean basement (greenstone-granite to the north and gneiss to the south) affected the manner of sedimentation and deformation. According to this model the greenstone-granite and gneiss terranes probably behaved as stable and unstable platforms, respectively. Sims (1976) suggested that plate tectonic systems characteristic of the Phanerozoic had not yet developed at this time. In contrast, Van schmus (1976) proposed a plate tectonic model, and explained the Chocolay and Menominee groups as miogeosynclinal deposits on a south-facing slope in an active collisional margin with an island arc and back-arc basin. During Menominee deposition, deformation apparently raised a submarine barrier to the south producing, shallow basins. The Baraga and Paint River groups are eugeosynclinal sediments deposited in a rapidly subsiding environment. According to this model, ocean floor was being subducted beneath the continental margin toward the north (Fig. 2a).

The arc-continent collision model was proposed by Cambray (1978). This model proposed that the Chocolay group was deposited in a cra-

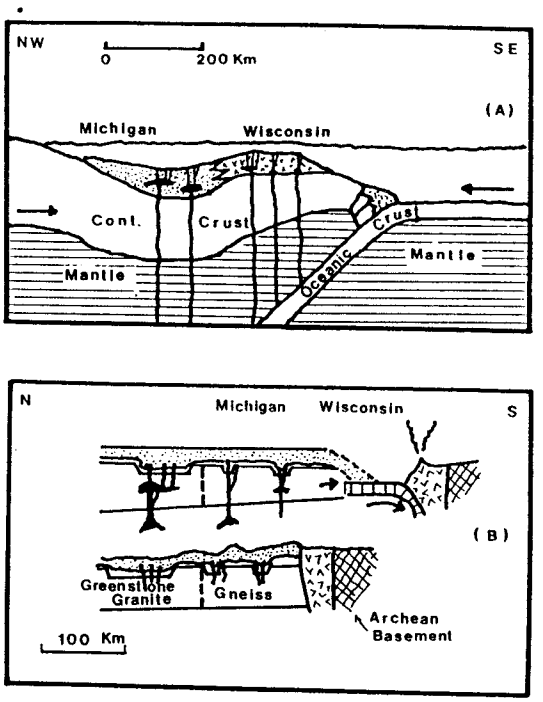

Fig. 2. Various plate tectonic models to explain the tectonic evolution of the Southern Lake Superior region. a) A reconstruction of the margin of the Archean craton about 1.9 Ga ago during the early stage of the Penokean Orogeny (Van Schmus, 1976). b)Schematic diagram showing plate-tectonic evolution of the Southern Lake Superior region (Larue and Sloss, 1980, model after Cambray, 1978). 1. Baraga Group sedimentation. 2. Collision with Cordilleran-type continental margin on southern magmatic arc complex.

tonic setting and that the strata of the Menominee group show features which are inferred to indicate initiation of rifting. According to this model the Penokean Orogeny represents the collision of a northern continent with an arc to the south. In contrast to Van Schmus (1976), Cambray postulated a southward-dipping subduction zone

SAMPLING AND ANALYTICAL METHODS

Fifty-three samples from the mafic dikes were analysed for major, trace, and rare earth elements. Standardized X-ray fluorescense (XRF) and Instrumental Neutron Activation Analyses (INAA) procedures developed at Michigan State University were used to determine whole rock compositions of the major, trace elements, and REE. Results of chemical analyses are listed in Table 1.

Major and selected trace elements were analyzed by a Rigaku (S-Max) automated X-ray fluorescence spectrometer. Glass waffles (for major elements) were made by the following procedure: 1) 1.0000 gram of crushed sample, 9.0000 grams of lithium tetraborates (flux), and 0.160 grams of ammonium nitrate (oxidant) were mixed with a spatula in Pt-Au crucibles, 2) this preparation was heated and gently shaken at approximatly 1100℃ for 20 to 30 minutes in orde 'o make a homogeneous liquid, 3) this liquid was then poured into a Pt-Au mold and

Table 1. Chemical Compositions.

Sample	Po-1	MR-1	MR-2	GR-1	GR-2	GR-3A	GR-3B	GR-4	MG-1	NRP-2	NRP-5	IP-1	IP-2	IP-3	IP-4
SiO_2	48.30	51.56	49.52	45.81	48.53	50.17	50.35	49.11	48.28	53.27	49.16	46.78	50.58	45.78	46.42
TiO_2	2.41	2.26	1.75	1.92	2.74	0.78	0.63	2.45	3.53	2.52	1.42	1.20	1.12	1.28	1.11
Al_2O_3	13.74	12.51	12.89	14.30	17.33	13.19	14.64	13.63	14.52	12.56	15.23	15.52	15.27	15.16	15.62
FeO	13.05	14.81	14.38	12.97	11.08	10.97	10.63	11.98	16.98	15.76	11.93	11.02	10.71	10.93	10.64
MnO	0.19	0.22	0.23	0.23	0.19	0.18	0.17	0.18	0.27	0.24	0.20	0.21	0.22	0.13	0.15
MgO	8.02	4.54	6.25	10.56	4.61	9.73	8.95	3.81	3.73	2.46	6.56	7.82	6.62	6.78	8.79
CaO	4.65	7.98	9.64	7.03	8.09	8.40	9.91	7.06	3.52	4.18	10.38	10.16	11.27	7.55	7.73
Na_2O	2.39	2.59	1.63	1.77	3.81	2.36	1.97	3.87	0.37	3.11	2.00	1.76	2.28	1.46	3.21
K_2O	1.39	1.07	0.77	1.53	1.10	0.31	0.79	1.45	4.90	2.26	1.06	0.46	0.44	2.10	0.85
P_2O_5	0.27	0.22	0.16	0.13	0.50	0.06	0.05	0.57	0.56	1.16	0.15	0.12	0.11	0.12	0.05
Total	94.41	97.76	97.22	96.25	97.98	96.15	98.09	94.11	96.66	97.52	98.09	95.05	98.62	91.29	94.57
Cr(X)	254.4	68.0	119.4	412.2	197.7	701.0	685.2	21.7	32.0	24.3	156.7	194.6	22.8	123.8	392.9
Ni	46.6	30.2	39.8	214.3	59.4	190.3	173.8	0.0	0.0	0.0	96.0	17.07	69.3	93.8	151.7
Cu	227.9	41.4	61.0	23.4	16.6	12.2	21.9	28.0	13.9	12.5	112.0	73.6	134.3	69.9	44.2
Zn	82.5	117.4	102.1	112.3	120.3	86.5	77.0	133.9	183.0	164.9	93.7	88.0	57.2	93.8	70.6
Rb	10.4	27.6	17.4	51.7	33.6	4.5	28.8	19.3	87.0	56.3	55.6	7.1	8.2	26.6	19.2
Sr	87.7	238.4	230.5	260.5	342.2	115.4	172.7	379.1	105.8	273.5	229.8	270.1	191.0	134.7	231.6
Y	27.8	29.8	27.3	24.4	32.6	14.9	17.6	40.0	35.6	54.5	26.5	18.3	21.7	18.8	17.6
Zr	155.7	179.3	111.2	109.1	229.6	70.1	56.7	293.0	271.0	438.9	103.2	104.4	81.1	90.7	57.2
Nb	20.4	18.2	8.9	21.7	16.7	5.6	2.8	57.0	29.3	65.6	10.1	7.2	3.7	8.5	7.7
Le(X)	12.20	25.50	13.00	17.30	30.50	6.80	4.20	34.20	32.70	67.10	7.30	12.30	16.40	12.90	0.50
Ba	255.5	365.0	155.2	384.2	554.3	18.6	93.4	484.8	1015.5	2130.0	361.5	213.7	154.4	411.9	363.0
La	15.38	29.93	9.89	14.33	32.56	10.96	8.43	39.51	55.31	87.11	13.18	11.77	5.49	10.46	7.04
Ce	23.14	24.16	12.82	35.25	69.52	26.94	24.83	115.51	116.10	146.38	23.47	28.51	18.03	25.93	9.58
Sm	5.13	6.86	4.19	3.53	6.88	3.54	2.53	8.03	10.81	16.19	3.82	3.18	2.55	3.17	1.54
Pu	1.86	1.97	1.83	1.33	2.14	1.43	1.37	4.12	2.99	4.59	1.61	1.27	0.95	1.10	1.24
Tb	1.00	0.96	1.04	0.57	0.81	0.77	0.73	0.71	0.91	1.04	0.89	0.51	0.53	0.56	0.77
Yb	2.60	2.51	2.70	1.91	2.69	2.37	2.27	2.57	2.30	2.56	2.34	1.89	1.89	1.48	2.11
Lu	0.46	0.46	0.51	0.30	0.44	0.35	0.34	0.36	0.41	0.46	0.39	0.31	0.39	0.19	0.39
Rf	3.54	3.50	3.48	2.88	6.01	6.11	4.64	11.09	3.87	4.84	6.50	2.63	2.33	2.41	2.51
Th	8.30	10.43	10.18	1.86	6.05	7.00	4.84	5.61	9.80	11.70	9.38	1.87	1.42	2.05	4.64
Cr	236.9	119.6	170.9	380.3	154.3	603.9	602.9	44.5	89.3	93.5	170.2	158.3	229.6	84.3	263.1
Sc	45.0	38.4	43.8	24.0	43.8	34.9	32.3	32.9	27.2	29.9	37.3	30.8	40.9	27.9	33.7
FeO_2	13.05	14.81	14.38	12.97	11.08	10.97	10.63	11.98	16.98	15.76	11.93	11.02	10.71	10.93	10.64
F/F+M	0.623	0.768	0.700	0.556	0.710	0.534	0.547	0.761	0.822	0.867	0.649	0.590	0.623	0.620	0.550
Rb/Sr	0.119	0.116	0.075	0.198	0.098	0.039	0.167	0.051	0.822	0.206	0.242	0.026	0.043	0.197	0.083
X/Rb	1109	322	367	245	272	572	228	624	467	333	158	538	445	655	367
X/B8	45.2	24.3	41.2	33.1	16.5	138.3	70.2	24.8	40.0	8.8	24.3	17.9	23.7	42.3	19.4
den	2.70	2.71	2.74	2.75	2.67	2.69	2.69	2.66	2.72	2.66	2.70	2.72	2.69	2.69	2.69

transferred to a hot plate for annealing, which was then removed and allowed to cool to room temperature. The trace elements Rb, Sr, Nb, Y, Cr, Ni, Cu, Zn, Zr, and Y were also analyzed by XRF, using pressed powder pellets, with a sample/cellulase (Amercil) binder ratio of 4: 1. REE and Cr, Th, Sc, and Hf were analyzed by INAA. Powdered 1.00000 gram (>200 mesh) samples were sealed in polyvinyl vials and irradiated for 18 hours over a 3 day period. The short lived isotopes, La, Sm, and Sc were analyzed after 5 to 7 days and other elements were analyzed after 2 weeks from irradiation.

Accuracy for major elements is within 2% except for P, which is 5.4%. Trace elements by XRF are accurate to within 5% except for Y and Zn, which are less than 10%. Accuracy for elements by INAA is less than 10%, but where concentrations are less than 10 ppm (Tb, Lu, and Th), accuracy approaches 15%

PETROGRAPHY

The mineralogy and texture of the dikes vary widely through the area. The dikes consist predominantly of amphibole (primarily hornblende), plagioclase, biotite, chlorite, and a vari-

Table 1. Continued.

Sample	SQ-2B	SQ-3A	SQ-3B	NSW-1	NS-1	RP-1	RP-2B	RP-2A	RP--3	RP-4	NG-2	Rp-5	Ns-3	Wf-1	Wf-2
SiO_2	48.49	48.32	49.58	49.09	49.38	55.03	51.40	52.75	51.65	50.40	48.53	52.14	44.98	50.79	51.24
TiO_2	3.36	1.49	1.58	1.30	1.07	2.37	0.82	0.69	1.16	2.53	1.83	2.12	0.83	2.28	1.60
Al_2O_3	12.87	13.86	14.25	15.50	13.39	15.33	13.67	13.20	13.70	13.47	14.25	13.97	15.68	12.44	13.49
PeO	16.79	14.38	13.39	10.61	15.02	12.86	12.93	9.43	12.53	12.23	11.82	12.06	12.69	14.59	13.15
MnO	0.18	0.18	0.21	0.18	0.17	0.23	0.21	0.16	0.23	0.19	0.17	0.17	0.20	0.22	0.21
MgO	4.22	6.89	7.21	8.10	7.63	2.57	6.31	8.99	7.04	5.79	7.82	5.24	11.64	4.84	5.48
CaO	6.89	4.55	4.13	7.92	6.05	4.53	10.15	9.87	9.72	9.56	9.62	7.68	6.47	8.51	6.67
Na_2O	2.29	3.32	3.91	3.04	3.19	3.66	2.22	2.36	1.66	2.42	2.22	2.47	2.35	1.71	3.16
K_2O	1.18	1.01	0.89	1.20	0.92	1.70	0.67	0.93	0.60	1.60	0.53	1.85	0.46	1.32	2.21
P_2O_5	0.40	0.15	0.12	0.12	0.08	0.47	0.09	0.06	0.13	0.25	0.21	0.25	0.06	0.31	0.19
Total	95.67	94.15	95.27	97.06	96.90	98.75	98.47	98.44	98.42	98.45	97.00	97.95	95.36	97.01	97.40
Cr(X)	123.8	138.6	178.4	405.0	92.5	35.1	116.4	491.4	222.5	119.9	272.8	75.7	242.8	75.2	76.3
Ni	55.0	61.8	80.5	87.0	50.7	0.0	69.1	158.2	66.2	39.6	60.3	31.8	440.3	33.4	39.5
Cu	108.1	126.8	139.8	15.6	14.2	7.5	46.1	85.1	65.7	35.0	65.2	52.7	205.9	87.8	71.9
Zn	96.4	131.2	127.2	90.5	88.2	112.6	103.6	95.4	119.7	109.3	86.1	121.7	102.9	121.4	115.6
Rb	26.9	25.0	16.4	14.8	22.7	49.0	14.5	63.3	21.8	57.0	13.6	101.4	11.2	35.1	47.9
Sr	335.1	107.8	139.2	350.3	156.4	215.9	175.5	166.5	119.2	301.9	358.8	371.8	120.2	185.2	255.8
Y	35.9	30.2	25.0	15.5	21.1	49.5	19.1	22.3	26.3	27.6	18.9	36.8	15.9	31.9	28.6
Zr	236.8	129.6	104.8	82.8	62.0	309.3	76.0	66.4	89.0	167.2	109.4	276.3	50.1	167.0	143.1
Nb	10.3	8.1	5.8	6.7	3.1	84.4	3.2	3.8	10.1	23.2	9.3	42.7	3.2	20.6	13.3
La(X)	26.80	17.10	8.20	9.20	1.60	54.10	10.80	3.60	11.90	20.60	14.00	49.50	2.00	25.50	20.60
Ba	2008.4	407.7	222.7	566.3	227.5	925.8	55.0	109.6	130.8	299.4	228.3	607.8	82.4	409.40	632.2
La	20.99	12.99	10.03	17.85	7.01	62.62	9.39	9.90	12.16	22.56	14.96	62.41	4.64	22.14	23.09
Ce	49.94	31.14	27.13	25.47	11.99	174.54	24.56	24.17	20.45	26.65	28.42	119.24	9.96	56.61	48.97
Sn	9.18	4.69	4.43	4.72	1.77	10.48	3.36	3.23	3.88	6.63	4.45	9.39	1.37	6.29	4.88
Bu	2.90	1.37	1.30	2.00	1.60	6.07	1.48	1.19	2.15	2.90	2.61	2.69	1.32	1.88	1.66
Tb	0.85	0.45	0.52	0.70	1.05	0.74	0.75	0.71	0.95	0.86	0.75	0.85	0.82	0.74	0.76
Yb	3.31	3.06	2.70	2.23	2.76	2.85	2.41	2.20	2.44	2.25	2.41	2.65	2.15	2.90	2.39
Lu	0.47	0.52	0.46	0.36	0.47	0.38	0.37	0.34	0.40	0.36	0.37	0.34	0.37	0.44	0.40
Hf	6.55	3.28	2.76	5.07	3.24	14.10	5.22	3.75	6.78	6.92	6.96	7.48	5.89	4.42	3.99
Th	3.18	2.36	1.71	4.18	10.31	8.05	5.75	4.58	9.19	8.33	5.24	10.43	6.22	5.06	6.21
Cr	119.2	93.0	103.3	340.4	158.7	43.8	127.9	478.7	216.7	140.1	301.5	95.9	243.0	40.5	54.4
Sc	36.1	35.8	40.2	40.6	48.1	37.6	32.9	33.9	38.7	32.6	34.2	27.4	36.4	40.0	35.3
F/F+M	0.801	0.679	0.654	0.571	0.666	0.836	0.676	0.516	0.644	0.682	0.605	0.700	0.525	0.754	0.709
Rb/Sr	0.080	0.232	0.118	0.042	0.145	0.227	0.083	0.380	0.183	0.189	0.038	0.273	0.093	0.190	0.187
K/Rb	364	335	450	673	336	288	384	122	228	233	323	151	341	312	383
K/Ba	4.9	20.6	33.2	17.6	33.6	15.2	101.1	70.4	38.1	44.4	19.3	25.3	46.3	26.8	29.0
den	2.76	2.70	2.68	2.67	2.72	2.62	2.70	2.66	2.70	2.69	2.72	2.66	2.75	2.72	2.67

able amount of oxide minerals. Other minerals present are epidote, clinozoisite, quartz, carbonate, and apatite as a minor phase. Some samples show a well developed orientation of hornblende and biotite grains. Diabasic texture is often found with almost complete alteration of pyroxene to hornblende.

Feldspar: The predominant feldspar may be plagioclase of andesine-labradorite composition and /or orthoclase. Plagioclase generally occurs as subhedral to anhedral, fine to medium, grains which comprise from 15% to 50% of the rock. Sericitization of plagioclase is very common and, in some cases, grains are partially replaced by carbonate. Inclusions of biotite, hornblende, and apatite are very common.

Amphibole: Most of the dikes have a varying amounts of hornblende (10% to 50%) with mostly anhedral to subhedral shapes. They often show twinning and inclusions. They are, in some cases, altered to chlorite and biotite. Some samples show a tremolite composition and, in some cases, fibrous actinolite is present. Based on the color, two different types of hornblende are recognized. One is dark green and faintly blue, and other is a blue green variation. The different colors in hornblende are usually caused by the change in the Fe^{3+}/Fe^{2+} ratio,

Table 1. Continued.

Sample	IP-5	IP-6	WL-1	WL-2	WI-4	MQ-1A	MQ-1B	MQ-1C	MQ-4	RQ-1	RQ-2	SQ-1A	SQ-1B	SQ-1	SQ-2A
SiO_2	47.38	49.15	51.37	54.73	51.22	48.83	48.72	48.94	52.40	48.26	50.89	49.68	49.11	49.67	46.42
TiO_2	0.95	2.54	0.72	0.76	1.96	2.41	2.38	2.22	0.65	2.09	2.83	1.19	1.23	1.14	3.49
Al_2O_3	16.60	13.89	16.03	15.98	12.67	12.93	13.19	13.38	15.26	14.45	12.48	14.06	13.54	13.94	13.68
FeO	9.30	16.67	10.33	11.53	15.59	15.07	14.98	14.98	8.61	11.85	16.08	13.84	14.16	13.49	17.63
MnO	0.15	0.19	0.21	0.16	0.19	0.19	0.19	0.15	0.16	0.19	0.25	0.22	0.22	0.21	0.29
MgO	9.02	3.97	7.95	5.75	5.54	6.01	6.05	6.30	7.53	5.93	2.92	6.38	6.44	6.77	5.31
CaO	8.90	3.39	6.35	2.77	6.22	6.11	7.27	4.12	8.43	11.28	7.16	8.99	9.69	9.26	1.28
Na_2O	2.52	3.14	4.48	1.57	1.88	2.52	2.52	4.11	3.14	2.14	3.07	1.94	1.81	2.18	0.75
K_2O	0.72	1.23	0.39	3.77	1.03	1.19	1.50	1.40	0.64	1.81	1.67	1.04	0.88	0.72	5.44
P_2O_5	0.04	0.89	0.06	0.07	0.22	0.19	0.17	0.19	0.06	0.22	1.33	0.11	0.12	0.11	0.41
Total	95.58	95.06	97.89	97.09	96.52	95.45	96.97	95.79	96.88	98.22	98.68	97.45	97.20	97.49	94.70
Cr(X)	426.9	16.5	229.3	293.0	92.4	98.9	105.4	115.0	148.7	119.6	52.4	110.0	122.2	141.4	139.3
Ni	219.8	0.0	100.8	92.4	21.6	48.1	51.9	57.2	61.5	40.8	1.2	92.1	85.9	101.2	94.9
Cu	75.6	12.7	228.4	0.0	183.6	46.9	66.0	54.6	232.1	19.9	8.1	142.3	160.9	130.3	203.2
Zn	69.0	153.8	78.5	101.6	104.4	112.2	114.1	117.6	68.9	110.1	155.1	98.8	130.1	99.9	135.9
Rb	16.5	13.1	1.6	135.8	23.7	24.6	40.8	64.2	10.2	28.2	46.7	35.2	48.2	25.0	78.5
Sr	190.2	62.7	136.2	59.1	84.5	516.1	388.3	229.2	146.7	325.8	248.0	138.2	125.4	157.3	102.2
Y	17.8	40.8	16.9	34.9	29.1	20.9	22.9	26.2	16.5	20.1	53.8	25.9	26.9	24.5	42.2
Zr	54.9	313.2	52.4	50.7	144.6	138.3	125.0	121.1	64.6	128.0	380.6	91.7	87.8	89.5	236.8
Nb	5.9	60.2	6.3	5.9	14.3	4.0	5.0	7.6	3.0	15.3	70.3	5.4	5.8	6.2	17.1
Le(X)	4.20	41.90	7.90	7.10	14.50	8.50	10.90	13.20	5.90	22.90	69.30	15.70	12.50	11.90	25.30
Ba	195.7	123.6	25.6	279.6	387.8	941.5	491.8	558.1	157.7	614.6	1197.2	163.7	124.1	190.4	789.9
La	7.78	52.90	13.40	6.90	17.97	18.73	15.78	16.32	6.09	20.02	76.08	8.44	9.41	10.00	20.06
Ce	9.72	110.36	18.86	12.53	23.57	20.65	20.65	20.40	13.07	21.13	143.81	24.41	27.29	23.93	50.50
Sn	1.64	13.72	1.97	1.88	5.21	5.23	4.99	4.70	2.16	4.87	14.70	3.71	3.79	3.51	8.16
Eu	1.26	4.17	1.44	0.81	1.99	1.85	1.78	1.75	0.72	2.31	4.52	1.16	1.22	1.17	2.44
Tb	0.77	0.80	0.91	0.38	1.05	0.90	0.90	0.90	0.41	0.84	1.06	0.34	0.65	0.61	0.72
Yb	2.11	2.08	2.42	1.77	2.75	2.35	2.35	2.40	1.94	2.69	2.58	2.36	2.80	2.60	3.19
Lu	0.38	0.39	0.40	0.30	0.48	0.42	0.41	0.42	0.32	0.34	0.46	0.38	0.41	0.44	0.45
Hf	2.51	3.72	6.22	1.17	3.66	2.03	3.15	3.13	1.48	6.50	4.68	1.87	2.73	2.10	6.12
Tb	5.21	9.30	8.31	1.01	11.13	9.41	9.28	9.34	1.27	7.59	11.56	1.57	1.90	1.89	2.46
Cr	329.3	60.7	223.6	251.9	143.0	135.4	135.4	138.2	117.8	134.7	96.7	95.4	83.8	109.1	111.0
Sc	33.6	19.3	41.4	39.3	41.8	36.2	36.1	36.3	38.4	34.2	31.3	40.6	40.7	39.7	33.9
F/F+M	0.512	0.809	0.570	0.670	0.740	0.717	0.715	0.706	0.538	0.670	0.848	0.688	0.691	0.669	0.771
Rb/Sr	0.087	0.209	0.012	0.298	0.280	0.048	0.105	0.280	0.070	0.087	0.188	0.255	0.384	0.159	0.768
K/Rb	362	779	2023	230	361	402	305	181	521	533	291	245	152	239	575
K/Ba	30.5	82.6	126.4	111.9	22.0	10.5	25.3	20.8	33.7	24.4	11.6	52.7	58.9	31.4	57.2
den	2.68	2.71	2.64	2.59	2.72	2.73	2.73	2.70	2.62	2.71	2.71	2.72	2.73	2.72	2.73

Table 1. Continued

Sample	WF-3	WP-4	WP-5	WP-6A	WP-6B	WP-7A	WP-B
SiO_2	54.46	43.37	51.22	49.47	49.39	48.10	47.38
TiO_2	2.00	3.33	1.57	1.96	1.96	3.15	1.74
Al_2O_3	12.36	14.97	13.06	12.52	12.52	11.50	14.61
FeO	13.92	21.36	13.56	13.52	16.08	12.72	13.38
MnO	0.21	0.09	0.22	0.26	0.25	0.18	0.22
MgO	3.52	6.14	5.82	5.15	5.54	7.64	6.82
CaO	4.31	0.67	8.62	9.62	9.63	9.92	8.98
Na_2O	2.18	0.00	2.65	1.75	2.08	2.88	2.91
K_2O	3.36	5.35	1.19	1.07	0.64	0.64	1.12
P_2O_5	0.37	0.43	0.14	0.19	0.17	0.30	0.17
Total	96.69	95.71	98.05	97.51	97.26	97.03	97.33
Cr(X)	41.1	48.9	93.5	109.5	114.2	330.1	133.9
Ni	0.8	28.8	45.7	38.4	45.2	144.4	65.4
Cu	29.0	68.2	92.0	172.9	161.8	140.4	107.5
Zn	113.0	99.6	114.6	124.5	119.5	113.6	99.6
Rb	63.9	79.6	45.7	46.3	21.4	15.2	32.7
Sr	146.4	28.9	240.6	188.9	167.7	617.8	216.1
Y	43.2	39.9	26.9	33.1	28.5	24.4	23.2
Zr	249.9	216.8	113.4	122.9	112.8	288.5	91.6
Nb	27.5	29.4	8.9	18.2	16.9	22.7	12.6
La(X)	39.70	30.60	18.00	11.80	17.30	39.0	12.30
Ba	1186.40	714.60	271.80	339.00	293.40	253.40	535.10
La	35.60	29.90	14.47	19.15	16.06	40.71	12.85
Ce	90.01	84.79	36.34	25.31	25.22	101.26	22.30
Sn	8.54	8.44	4.11	5.31	5.03	10.24	3.27
Bu	2.43	1.86	1.29	2.04	1.97	3.13	2.34
Tb	1.21	1.22	0.66	1.14	1.14	0.84	1.02
Yb	3.83	3.39	1.93	2.95	2.90	2.15	2.67
Lu	0.52	0.46	0.36	0.52	0.52	0.36	0.47
Hf	7.12	6.55	2.99	3.72	3.70	7.82	3.31
Th	11.06	9.99	2.74	11.45	11.80	8.81	10.27
Cr	6.9	9.3	66.0	175.0	192.3	279.2	181.0
Sc	30.2	43.3	45.0	46.7	50.6	27.4	44.2
F/F+M	0.801	0.777	0.703	0.754	0.735	0.628	0.666
Rb/Sr	0.436	2.754	0.190	0.245	0.128	0.025	0.151
K/Rb	436	558	216	192	248	349	284

which reflects changes in metamorphic conditions, especially in temperature. With increasing metamorphism, the H_2O content and the Fe^{3+}/Fe^{2+} ratio tend to decrease (Miyashiro, 1968) and the color changes from blue to green and green to brown. It is likely, therefore, that the blue hornblende represent a lower grade metamorphism than green ones.

Pyroxene: A few samples exhibit pyroxene as optically-discontinuous cores of hornblende plates. They are colorless with a birefringence of 0.020 - 0.036 and are augitic in composition.

Biotite: Biotite occurs in most samples in the high metamorphic grade zones, and occurs as replacement of hornblende. Primary augite was seen in some samples from the Wakefield quadrangle. Most of them have been altered to hornblende.

Chlorite: Chlorite is present in nearly all samples in varying amounts (trace to 15%). It usually occurs as aggregats of fine shreds and alteration products of hornblende and biotite.

Mineral assemblages are consistent with the greenschist and amphibolite facies of metamorphism. Low grade mineral assemblages in some dikes, such as plagioclase + chlorite + epidote + (carbonate) or plagioclase + actinolite + epidote + (carbonate) indicate a typical greenschist facies. Dikes with assemblages such as plagioclase + hornblende + (epidote) or pla-

gioclase + hornblende + biotite + (epidote, chlorite) indicate a higher grade metamorphism typical of the amphibolite facies.

GEOCHEMISTRY

Major Elements

The analyzed dikes have mostly basaltic compositions with a relatively wide range of SiO_2 (43-60 %) and are mostly quartz normative. A few samples are nepheline normative, possibly caused by the addition of Na and K during hydrothermal alteration or metamorphic recrystallization (Knoper and Condie, 1988). Dikes have tholeiitic affinities based on Irvine and Baragar's (1971) classification scheme. These rocks have relatively low Mg number (MgO/MgO + FeO) which indicate that significant fractionation of the rocks, and such evolved compositions are typical of Precambrian intrusive rocks from other localities (Condie et al., 1987).

Sun and Nesbitt (1978) suggested the use of CaO/TiO_2 and Al_2O_3/TiO_2 versus TiO_2 plots to separate different magma types. Fig. 3 shows the Al_2O_3/TiO_2 and CaO/TiO_2 plots of the rocks from the magmatic arc terrane (data from Cudzilo, 1978) and northern passive margin terrane. The low-Ti calc-alkaline rocks from the magmatic arc terrane have extremely high Al_2O_3/TiO_2 and CaO/TiO_2 ratios whereas the relatively high-Ti tholeiitic basalts from the northern passive margin terrane have lower Al_2O_3/TiO_2 and CaO/TiO_2 ratios (less than 20). The ratios increase with increasing degree of source melting that results in a progressive decrease of Al_2O_3/TiO_2 and CaO/TiO_2 in the residual mantle. Sun and Nesbitt (1978) noted that these ratios level off and remain constant at a critical value, irrespective of the degree of melting. The maximum ratios in magma produced from the Mid-ocean ridges are close to those in chondrite (17 to 20) at approximately 0.8 % TiO_2 (Gaskarth and Parslow, 1987). Thus, the high-ratios could not be produced by an increasing degree of melting of any known mantle mineralogy and the depletion must be inherited from the source. One possible origin suggested for these high-ratio low TiO_2 basalts is remelting of a source which was severely depleted in incompatible elements by previous episodes of magma extraction.

Thus, high-Ti basalts are possibly similar to Mid-ocean ridge type, whereas low-Ti basalts are more analogous to modern basalts from island arc or interarc basin (Sun and Nesbitt, 1978; Gaskarth and Parslow, 1987). Based on

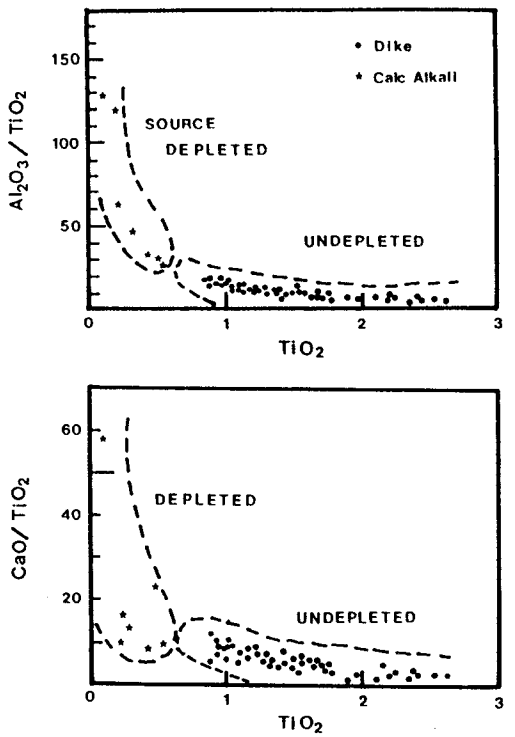

Fig. 3. Diagrams using TiO_2 to detect degree of depletion in the magma source (Sun and Nesbitt, 1978). Most of the rocks of Quinnesec Formation (data from Cudzilo, 1978) reside in the area marked for arc volcanism, indicating they originated from partial melting of residual mantle. The dikes, on the other hand, came from a less depleted mantle source. Legend: circle, dike; and star, Quinnesec Formation.

Fig. 3, it can be suggested that the dikes are similar to high-Ti MORB-like tholeiites derived from a relatively undepleted source.

Trace and Rare Earth Elements

Variation of trace elements with increasing magmatic differentiation for the dikes are indexed with mole percentage of FeO/ (FeO + MgO). Compatible elements, Ni and Cr, decrease with increasing differentiation, while the hygromagmatophile elements (Rb, Ba, Zr, Y, etc.) show a trend of enrichment with increasing differentiation. In this study, the LIL (large ion lithophile) elements of the rock suites show a much wider scattering and poorer correlation as compared to the tight clustering of the immobile elements (e.g., Zr, Y). This suggests that the immobile elements can be used for

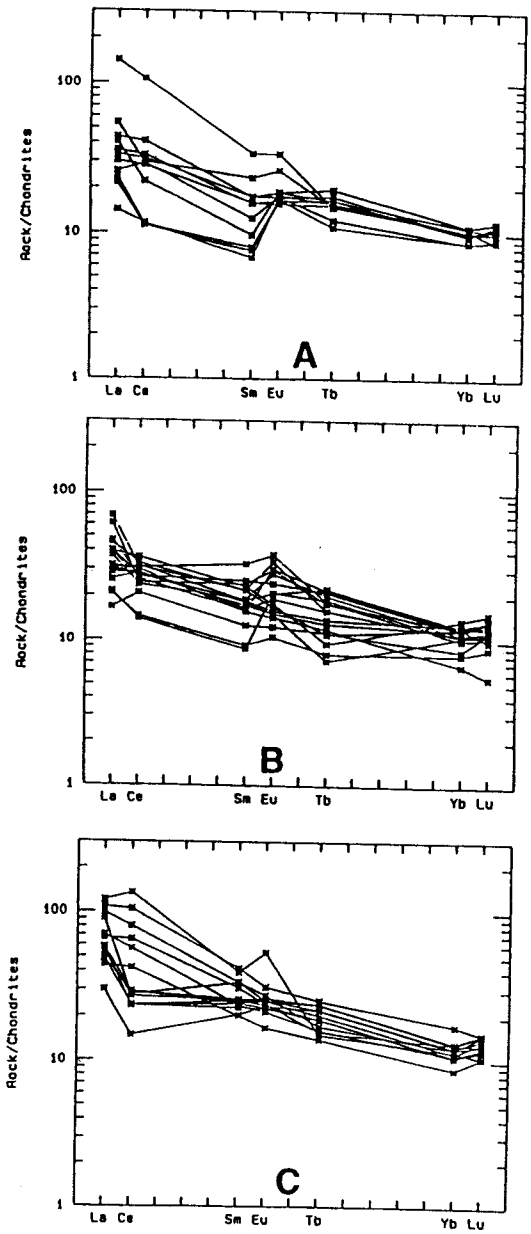

Fig. 4. Chondrite normalized REE patterns of the dikes. Samples are subgrouped based on FeO/(FeO + MgO) < 60 (a); 60 to 70 (b); and > 70 (c).

modelling whereas the LIL, whose scattering is problem due to alteration and metamorphism, may be used with caution. The REE concentrations were normalized to chondrite and then plotted logarithmically against atomic number

Fig. 4). Fig. is divided into three groups depending on degree of differentiation. REE distribution patterns show increasing LREE enrichment with increasing differentiation and most of the rocks exhibit LREE enrichment pattern. One of the less evolved rock has a high enrichment of LREE compared to HREE [$(La/Lu)_c$=15.7]. This excessive amounts of LREE in this less evolved sample can not be explained by magmatic processes. The possible causes of this enrichment might be a carbonitization or chloritization (Condie et al., 1977).

Spider diagrams for averages of the dike swarms and regional crustal rocks are shown in Fig. 5. This Figure shows enrichment of the LIL elements relative to the other incompatible elements. Depletion of Nb and P with respect to their neighboring elements suggest that the possibility of crustal contamination during magma emplacement.

INTERPRETATIONS OF TECTONIC SETTING

Different types of tectonic models have been proposed for the early Proterozoic tectonic environments of northern Michigan and northeastern Wisconsin (Cannon, 1973; Van Schmus, 1976; Cambray, 1978; Larue and Sloss, 1980; Larue and Ueng, 1985; Sims and others, 1980). One of the main objects of this research is to determine the tectonic environment of this

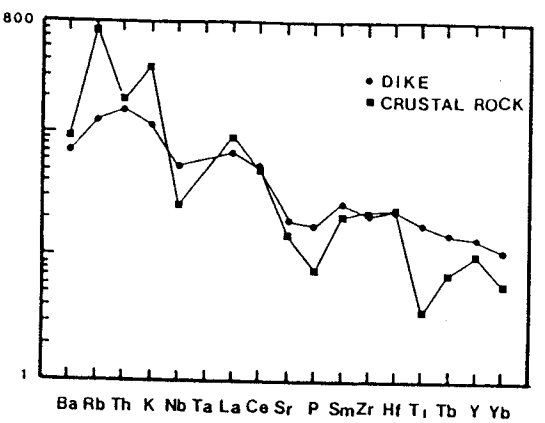

Fig. 5. Chondrite normalized geochemical patterns for the averages of the studied rock suites. For comparison, averaged crustal rocks are presented (data from this study and Ueng et al., 1988). Normalizing factors and arrangement of elements are based on Thompson (1982).

area by examining the trace element geochemistry of studied rocks. It has been recognized that volcanic rocks erupted within specific tectonic settings possess distinctive trace element and, in some cases, major element signatures.

A geochemical approach toward this goal is complicated by several factors. A major problem is interpreting the element abundances in the rock related to metamorphism. The rocks under investigation have suffered extensive metamorphism from the greenschist to amphibolite facies during the Penokean Orogeny. A series of well documented methods utilizing immobile elements are applied with caution in order to estimate the effects of mobilization.

Element Mobility

Pearce and Norry (1979) suggest that the Ti, Zr, Y, and Nb are not usually transported in aqueous fluids and thus these elements are unaffected by metamorphism through the greenschist facies (Cann, 1970). Muecke et al. (1979) show that the Ti, P, Y, Zr, Hf, and Nb are essentially unaffected by metamorphism to amphibolite facies. They concluded that the elements Ti, P, Zr, Hf, Ta, Sc, Nb, and Y in basalts are resistant to alteration and metamorphism, while other elements such as Sr, Ca, Ba, K, and Na can be shown to be mobile even during low grade alteration (Humphris and Thompson, 1978; Gelinas et al., 1982; Ludden et al., 1982).

Some research has reported REE mobility during submarine weathering and spilitization. Ludden and Thompson (1978, 1979) report that the LREE become enriched during seawater alteration but that the HREE show no selective mobilization. Wood et al. (1976) reported significant LREE mobility in zeolitized lavas from Iceland, but that high correlations of HREE with Ti, P, Zr, Ta, Hf, Y, and Nb indicated these elements were relatively unaffected. Both Frey et al. (1978) and Wood et al. (1976) mentioned alteration produced an irregular REE pattern and would therefore be recognized. Condie et al. (1977) studied the effects of alteration on Archean tholeiites and concluded that the LREE can be enriched if more than 10% carbonitization-chloritization occured but that up to 60% epidotization had no effect on the REE. Humphris et al. (1978) found little change in the REE in variously altered portions of individual basaltic flows, and they suggested that rock crystallization history would preferentially control REE mobility more than subsequent metamorphism. Muecke et al. (1979) suggested that metavolcanics up to amphibolite and granulite facies showed no REE mobility and strong correlation with previously mentioned immobile elements. In summary, it suggests that the elements such as Ti, P, Y, Zr, Hf, Nb, Ta, Sc, and HREE's in basalts are resistant to alteration and metamorphism, and these elements are suitable for use in a tectonic discrimination diagrams.

Test of Tectonic Setting Using Tectonic Discrimination Diagrams

In this study, previously devised tectonic discrimination diagrams were used in order to constrain the paleotectonic environment of the area. What these diagrams do not consider is the temporal decrease in global heat flow. This would have influenced the depth and degree of partial melting of the mantle and the likelihood of contamination by sialic crust. For above reasons, in the diagrams which follow, the field boundaries defined by modern volcanic rocks serve merely as a reference framework to which the Precambrian data can be compared.

Several discrimination schemes utilizing distinctive trace element distributions in mafic volcanics have been proposed to aid in the reconstruction of ancient tectonic settings. The application of such schemes to volcanic rocks of Precambrian age is based on the assumption that the ancient and modern chemical-tectonic systematics of magma genesis are basically the same.

a) Ti-Zr: Fig. 6 is a plot of Ti vs.Zr used by Pharaoh and Pearce (1984). The purposes of this diagram are 1) to identify which samples

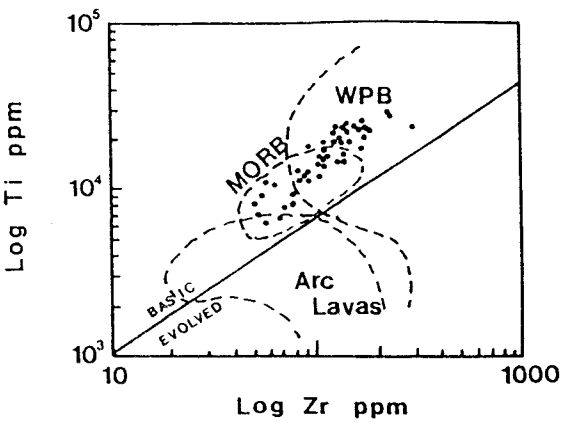

Fig. 6. Plot of Ti vs. Zr for the dikes. MORB, Within-plate, and Arc-volcanic field locations taken from Pharaoh and Pearce (1984).

are basic and thus able to be classified by basalt discrimination diagrams; and 2) to distinguish between a volcanic arc and a intraplate origin for the rocks. This diagram discriminates between basic and evolved lavas because the dominant crystallizing phases in basic magma (i.e., olivine, pyroxene, plagioclase) have an insignificant effect in the Ti/Zr ratio of the melt. However, when a Ti bearing phase begins to crystallize and the melt evolves from basic to acid, the removal of Ti results in a decrease in the Ti/Zr ratio (Watters and Pearce, 1987). In Figure 6, it is apparent that the all rocks fall in the basic lava side and that the majority of the rocks plot in the within plate basalt (WPB) field. Assimilation and Fractional Crystallization (AFC) processes do not significantly alter the tectonic indicators in the Ti-Zr plot (Ueng et al., 1988) because Zr concentrations are similar in the crustal material and the magmatic differentiates of the intermediate stage, and because the tendency to lower the Ti concentration of the magma by assimilating supracrustal rock is overshadowed by an enrichment trend caused by differentiation.

b) Ti-Zr-Y: Samples were plotted in Ti-Zr-Y (Pearce and Cann, 1973) to distinguish within plate basalt (WPB), ocean-floor basalt (OFB), low-K tholeiites (LKT), and calc-alkaline basalt (CAB) (Fig. 7). The WPB affinity of the rocks is a dominant feature of the plot. However, a fairly large number of rocks plot in the OFB fields. This kind of plot pattern has been interpreted by Morrison (1978) and Holm (1982) as representative of incipient spreading within continental crust. It thus appears that the basaltic rocks plot within and between WPB and OFB on this diagram and suggests that they have characteristic of continental basalts of transitional setting; either continental rifting or back arc basin.

c) Zr/Y-Zr: Figure 8 (Pearce and Norry, 1979), though not providing a complete separation of WPB and MORB, effectively distinguishes between these types and volcanic arc basalts. The rocks cluster mainly in the WPB field, with a few samples in the MORB field.

d) La/Nb Histogram: It is difficult to chemically distinguish the CTB and OIB with respect to degree of enrichment of overall elements. Both have enriched LIL and HFS elements, however, they show a distinctive difference in the concentration of Nb. Histograms of La/Nb ratio for examples of OIB, CFB, and subduction related basalts are given in Figure 9. Although this discriminant alone is insufficient to determine the paleotectonic environment of a single sample, it is adequate to distinguish between CFB, OIB, and IAB.

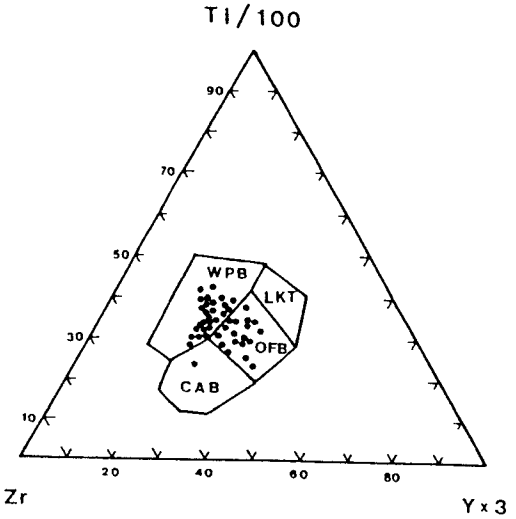

Fig. 7. Ti-Zr-Y diagram. Locations of basalt field are taken from Pearce and Cann (1973). WPB: within plate (intraplate) basalts, LKT: low-K tholeiitic basalts, OFB: ocean floor basalts, CAB: calc-alkaline basalts.

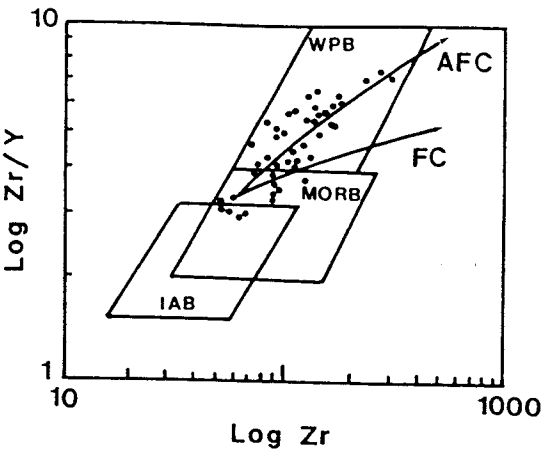

Fig. 8. Zr/Y vs. Zr diagram. Basalt field locations are taken from Pearce and Norry (1979). Line AFC marks the simulation of AFC differentiation path with R=0.35, OL:CPX:PL = 0.05:0.65:0.3. Line CF marks the differentiation path of a crystal fractionation model.

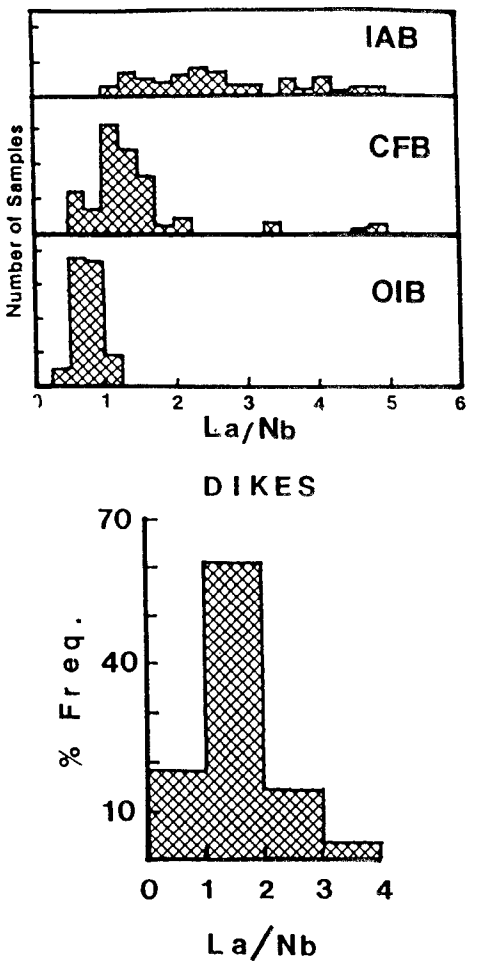

Fig. 9. Histogram of percent frequency vs. La/Nb. a) Histogram of La/Nb in island-arc basalts (IAB), continental flood basalts (CFB), and oceanic island basalts (OIB) (from Thompson et al., 1985). b) Histogram of La/Nb for the investigated rocks.

Comparisons of Geochemical Pattern to Suites of Known Tectonic Environment

MORB normalized geochemical patterns provide a useful means of comparing basalts based on the analyzed elements. Pearce (1982) proposed the use of N-MORB normalized LIL/HFS element distribution patterns to compare basalts. He used a comprehensive range of elements, including Sr, K, Rb, Ba, Th, Ta, Nb, Ce, P, Zr, Hf, Sm, Ti, Y, and Yb. LIL elements (Sr through Ba) in this list are relatively soluble in aqueous fluids, while the HFS elements (Th through Yb) are relatively immobile during metamorphism due to low solubility. Figure 10 illustrates some typical patterns of recent basalts of known tectonic environments normalized to N-type MORB (N-MORB data from Viereck et al., in press).

Basaltic rocks from back arc basin (Fig. 10a) exhibit 1) an enrichment in elements of low ionic potential and in Th, Ce, and P, characteristic of calc-alkaline basalts, and 2) an enrichment in all elements from Sr to Ti (except Nb) characteristic of intraplate tholeiites. The most obvious explanation for these patterns is that the mantle source regions have suffered at least two episodes of enrichment, one related to and the other unrelated to subduction (Pearce, 1982). The mantle source for these lavas seems to have undergone enrichment in K, Rb, and Ba, possibly resulting from dewatering of the subduction slab (Weaver et al., 1979). The lower absolute abundance of Nb is typical of back-arc basalt from the spreading center (Sanders et al., 1979). Selected modern suites of continental tholeiitic basalts (Fig. 10b) erupted in areas of strong lithospheric attenuation also give patterns which exhibit enrichment in the most incompatible elements and depletion in Nb and P with respect to their neighboring elements. The geochemical patterns of the basaltic rock groups from the study area (Fig. 10 c) have very similar distribution patterns and resemble the continental tholeiitic basalts in regard to the degree of enrichment of LIL/HFS elements and Nb and P depletion. The interpretation of these data strongly favor a model of intrusion into a crustal environment undergoing lithospheric attenuation.

The subduction related plate margin model (Van Schmus, 1976), in which the study area represents a back arc or foreland basin assemblage, seems suitable model for the area without consideration of the chemical characteristics of the rock suites. According to his model, the magma which supplied the dikes should be related arc volcanism, however, the geochemical characteristics of the rock suites are not associated with arc volcanism and show a lack of chemical characteristics of back-arc magmatism (Fig. 10a) but are comparable to rift zone tholeiitic basalts which was not related to subduction activity (Fig. 10b).

Based on the comparison of geochemical patterns of these suites to the known tectonic environments, these suites point to a tectonic setting in which tholeiitic magma was emplaced producing the dikes during rifting is

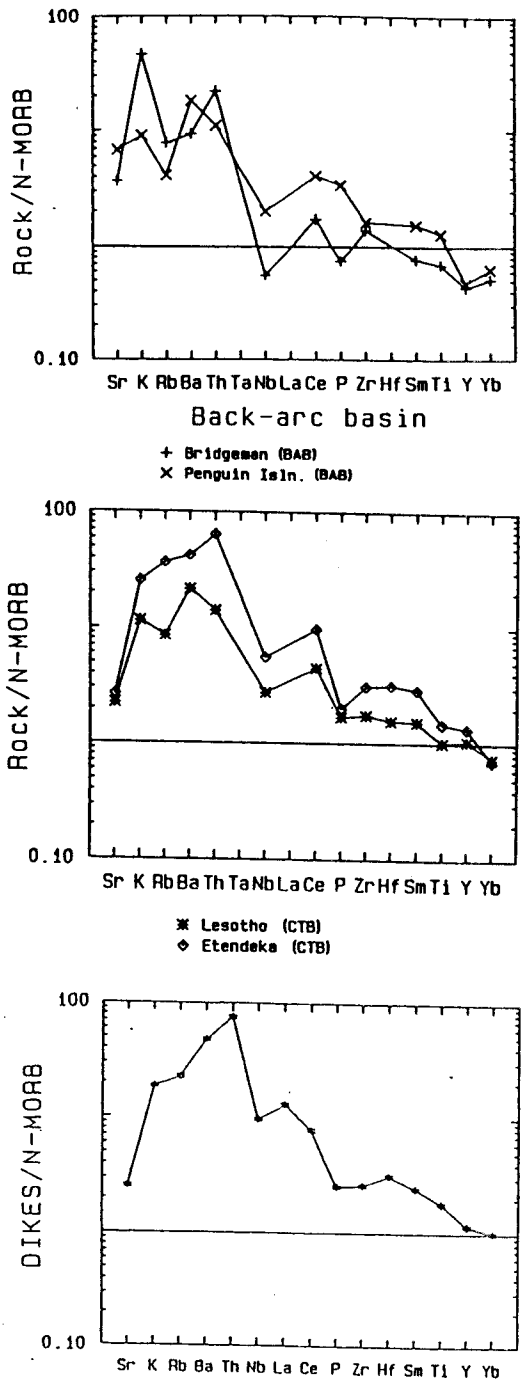

Fig. 10. Geochemical patterns of basalts from known tectonic environments normalized to N-type MORB. Data sources for Figure 10a cited in Weaver et al.(1979), 10b cited in Marsh (1987) and Peccerillo and Taylor (1976).

suggested. The geochemical patterns of the studied rock suites are analogous to the that of the lavas from the British Tertiary Volcanic Province (BTVP; Skye and Mull lavas; Brooks and Nielsen, 1982; Thompson, 1982) and to continental tholeiites from Edendeka in western Africa which erupted in a rift environment related to the separation of southern Africa from South America (Duncan, 1987). There are obvious similarities in geochemical patterns between rocks of the study area and those of the BTVP and Edendeka, both of which appear to represent rifted continental margin environments. Therefore, Cambray's (1978) model seems the most favorable to explain the tectonic evolution of the study area.

DISCUSSION

Based on Figures, most of the rocks from the study area plotted in either the WPB field or the MORB field. Of particular interest is that the less evolved rocks plot in the MORB field and evolved rocks show a trend into the WPB field as seen in the Zr/Y vs Zr plot. Although these diagrams do not provide a separation of normal MORB (N-type) and plume type MORB (P-type), chemical compositions of the least evolved samples are similar to that of transitional type MORB (T-type).

Recent studies of continental tholeiities, including the Deccan flood basalts of India, British Tertiary volcanics, Columbia River volcanics, and Precambrian Coppermine River basalts of Canada, have revealed that the elemental abundances and isotopic compositions of these rocks have been substantially modified by assimilation of the continental crust through which they erupt (Mahoney et al., 1982; Thompson, 1982; Brooks and Nielson, 1982).

The Zr/Y vs Zr plot (Fig. 8) show two differentiation paths; one is the Rayleigh crystal fractionation path (CF) and the other is assimilation fractional crystallization path (AFC). The latter represents the trend of assimilation in supracrustal rocks (Zr/Y > 10, data from Ueng et al., 1988) during differentiation of magma. Based on Figure 8, the AFC trend shows a good fit to the data.

Crustal contamination evidence for the studied dikes were reported based on field investigation (Wier, 1967). However, the extent of assimilation is very difficult to access for the basaltic dikes. In order to evaluate the effect of assimilation, the author has applied the equations proposed by DePaolo (1981) to simulate the REE variation in an assimilation-crystal fractionation model (Fig. 11). An

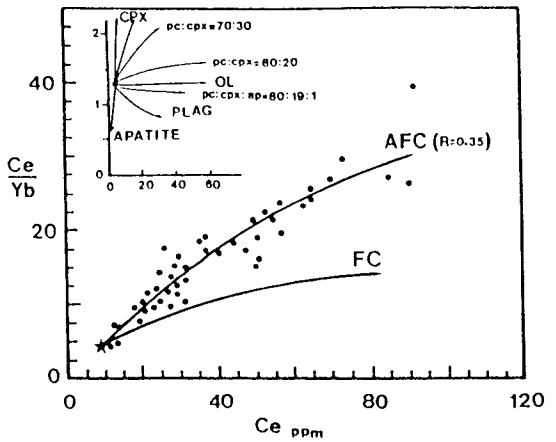

Fig. 11. Ce/Yb vs. Ce ppm plot for the dikes with FC and AFC models.

tion rate) of 0.35 was used here because the same number has been successfully applied in modeling the Deccan Basalt and the Coppermine River Basalt (Dupuy and Dostal, 1984). One dike sample (IP-5) is chosen to approximate the starting composition because of the following reasons; the low silica content (47%), high Mg value(63.4), high content of compatible elements (e.g., Ni=220 ppm, Cr=427 ppm), and the least differentiated REE compositions. As shown by FC (Rayleigh fractional crystallization) path shown in Figure 11, differentiation by simple fractional crystallization seems to have difficulty evolving the observed Ce/Yb ratios. The continental crust (Ce=60.0, Yb=3, Handerson, 1984) and supracrustal rocks (Ce=61.25, Yb=1.9, data from Ueng et al., 1988) have a higher Ce content and Ce/Yb ratios. It thus appears that the preferred processes to explain the excessive enrichment of Ce in the present study is AFC process.

In summary, these diagrams suggest that trace element distributions are related to AFC processes and that the source magma of the dikes are chemically not significantly different from T-type MORB compositions. Therefore, based on the trace element patterns and relative abundances, this study supports previous conclusions that the studied rocks are a result of a relatively undepleted parent magma (similar to present day T-type MORB) which was modified by crustal contamination. This shifted the composition to that of continental tholeiites as the rocks evolved.

CONCLUSION

Geochemical analysis, tectonic comparison using diagrammatic methods and limited chemical modeling of samples from the Precambrian dikes allow the following conclusions:

1) Despite the age and metamorphic grade of the area, geochemical analysis, especially for the immobile elements, has provided useful information and future chemical studies are encouraged.

2) The Precambrian dikes from the southern Lake Superior region are derived from a magma source which can be characterized as a high-Ti tholeiites similar to present day T-type MORB.

3) Assimilation crystal fractionation processes controlled the chemical differentiation of the magma. Assimilation of crustal rocks has affected the REE patterns, Ce/Yb and Zr/Y ratio, and contents of Nb and P.

4) Tectonic discrimination diagrams applied to these Precambrian dikes yield ambiguous results in comparison to modern tectonic analogs; liberal interpretations of these diagrams favor an extentional tectonic regime. Chemical criteria indicate that the magma was generated in a rifting environment similar to the early Tertiary opening of North Atlantic ocean.

REFERENCES

Baxter, D.A. and Bornhorst, T.J. (1988) Multiple discrete mafic intrusions of Archean to Keweenawan age, western Upper Peninsula, Michigan. (abstr.) 34th Annu. Inst. of Lake Superior Geol., Marquette, Michigan, p. 6-8.

Brooks, K.G. (1968) Magnetization of the lower most Keweenawan lava flows in the Lake Superior area. U. S. Geol. Surv. Prof. Paper 600-D, p. D248-D254.

Brooks, C.K. and Nielsen, T.F.D. (1982) The E. Greenland continental margins; a transition of continental to oceanic volcanism. J. Geol. Soc. of London, v. 139, p. 265-275.

Cambray, F.W. (1978) Plate tectonics as a model for the environment of deposition and deformation of the early Proterozoic (Precambrian X) of northern Michigan. Geol. Soc. Am. Abst. w/Prog., v. 10, no. 7, p. 376.

Cann, J.R. (1970) Rb, Sr, Y, Zr, and Nb in some ocean-floor basaltic rocks. Earth Planet. Sci. Lett., v. 10, p. 7-11.

Cannon, W.F. (1973) The Penokean Orogeny in Northern Michigan. Geol. Asso. Canada, Special Paper, v. 12, p. 251-271.

Cannon, W.F. (1975) Badrock geologic map of the Republic Quadrangle, Marquette County, Michigan. U. S. Geol. Survey, Misc. Investigations Series, Map I-862.

Cannon, W.F. and Gair, J.E. (1970) A revision of strati-

graphic nomenclature for middle Precambrian rocks in northern Michigan. Geol. Soc. Am. Bull., v. 81, p. 2843-2846.

Cannon, W.F., and Klasner, J.S. (1976) Geologic map and geophysical interpretation of the Witch Lake quadrangle, Marquette, Iron, and Baraga counties, Michigan. Misc. Geol. Investigation Map I-987.

Condie, K.C., Bobrow, D.J., and Card, K.D. (1987) Geochemistry of Precambrian mafic dikes from the southern Superior Province of the Canadian Shield. Geol. Soc. Canada Special Paper 34, p. 95-108.

Condie, K.C., Viljoean, M.J., and Kable, E.T.D. (1977) Effects of alteration on element distributions in Archean tholeiites from the Barberton Greenstone Belt, south Africa. Contrib. Mineral. Petrol., v. 64, p. 75-89.

Cudzilo, T.F. (1978) Geochemistry of early Proterozoic igneous rocks northeastern Wisconsin and upper Michigan. Ph.D. Thesis, University of Kansas, 202p.

DePaolo, D.J. (1981) Trace element and isotopic effects of combined wallrock assimilation and fractional crystallization. Earth Planet. Sci. Lett., v. 53, p. 189-202.

Duncan, A.R. (1987) The Karoo igneous province; a problem area for inferring tectonic setting from basalt geochemistry: In Tectonic controls on magma chemistry, edited by S.D. Weaver. J. Volcano. Geotherm. Res., v. 32, p. 13-34.

Dupuy, C. and Dostal, J. (1984) Trace element geochemistry of some continental tholeiites. Earth Planet. Sci. Lett., v. 67, p. 61-69.

Frey, F.A., Green, D.H., and Roy, S.D. (1978) Integrated models of basalt petrogenesis: a study of quartz tholeiites to olivine melitites from southeastern Australia utilizing geochemical and experimental petrological data. J. Petrol., v. 19, p. 463-513.

Gaskarth, J.W. and Parslow, G.R. (1987) Proterozoic volcanism in the Flin Flon greenstone belt, east central Saskatchewan, Canada, In: Pharaoh, T.C., Beckinsale, R.D., and Rickard, D (eds) Geochemistry and Mineralization of Proterozoic volcanic suites. Geol. Soc. Special Publication, no. 33, p. 183-200.

Gelinas, L., Mellinger, M., and Trudel, P. (1982) Archean mafic metavolcanics from the Rouyn-Noranda district, Abitibi Greenstone belt, Quebec. 1. Mobility of the major elements. Canadian J. Earth Sci., v. 19, p. 2258-2275.

Greenberg, J.K. and Brown, B.A. (1983) Lower Proterozoic volcanic rocks and their setting in the southern Lake Superior district. Geol. Soc. Am. Mem. v. 160, p. 67-84.

Henderson, P. (1984) General geochemical properties and abundances of the rare earth elements. In: Henderson, P. (ed) Rare earth element geochemistry. Elsevier, Amsterdam, p. 1-32.

Holm, P.E. (1982) Non-recognition of continental tholeiites using the Ti-Zr-Y diagram. Contrib. Mineral. Petrol., v. 79, p. 308-310.

Humphris, S.E. and Thompson, G. (1978) Trace element mobility during hydrothermal alteration of oceanic basalts. Geochim. Cosmochim. Acta, v. 42, p. 127-136.

Irvine, T.N. and Baraga, W.R.A. (1971) A guide to the chemical classification of the common volcanic rocks. Canadian J. Earth Sci., v. 8, p. 523-548.

James, H.L. (1958) Stratigraphy of pre-Keweenawan rocks in parts of northern Michigan. U. S. Geol. Survey Prof. Paper 314-C, p. 27-44.

James, H.L., Dutton, C.E., Pettijohn, F.J., and Weir, K. (1968) Geology and ore deposits of the Iron River-Crystal Falls district, Iron county, Michigan. U. S. Geol. Survey Prof. Paper 570, 134p.

Klasner, J.S. and Cannon, W.F. (1978) Badrock geologic map of the southern part of the Michigamme and Three Lakes quadrangles, Marquette and Baraga counties, Michigan. Misc. Geol. Investigation Map I-1078.

Knoper, M.W. and Condie, K.C. (1988) Geochemistry and petrogenesis of early Proterozoic amphibolites west-central Colorado, U. S. A., Chem. Geol., v. 67, p. 209-225.

Larue, D.K. (1983) Early Proterozoic tectonics of the Lake Superior region: Tectonostratigraphic terranes near the purported collision zone. Geol. Soc. Am. Mem. 160, p. 33-47.

Larue, D.K. and Sloss, L.L. (1980) Early Proterozoic sedimentary basins of the Lake Superior region: Summary. Geol. Soc. Am. Bull., Part I, v. 91, p. 450-452.

Larue, D.K. and Ueng, W.L. (1985) Florence-Niagara terrane, an early Proterozoic accretionary complex, Lake Superior region, U. S. A. Geol. Soc. Am. Bull., v. 96, p. 1179-1187.

Ludden, J.N. Gelinas, L., and Trudel, P. (1982) Archean metavolcanics from the Rouyn-Noranda district, Abitibi greenstone belt, Qubec. 2. Mobility of trace element and petrogenetic constraints. Canadian J. Earth Sci., v. 19, p. 2276-2287.

Ludden, J.N. and Thompson, G. (1978) Behavior of rare earth elements during submarine weathering of sea-floor basalt. Earth Planet. Sci. Lett., v. 43, p. 85-92.

Mahoney, J., Macdougall, J.D., Lugmair, G.W., Murali, A. V., Sankar Das, M., and Gopalan, K. (1982) Origin of Deccan Trap flows at Mahabaleshwar inferred from Nd and Sr isotopic and chemical evidence. Earth Planet. Sci. Lett., v. 60, p. 47-60.

Marsh, J.S. (1987) Basalt geochemistry and tectonic discrimination within continental flood basalt provinces. J. Volcano. Geotherm. Res., v. 32, p. 35-49.

Nelson, W.G. and Thompson, G. (1971) Petrology of a transform fault zone and adjacent ridge segments, In A discussion on the petrology of igneous and metamorphic rocks from the ocean floor. Phil. Trans. Royal Soc. London, Sreies A., v. 268, p. 423-441.

Miyashiro, A. (1968) Metamorphism of mafic rocks. In: Hess, H.H. (ed) Basalt v. 2. Interscience Publishers, New York, p. 799-834.

Morey, G.B. (1978) Metamorphism in the Lake Superior region, U. S. A., and its relation to crustal evolution.

Geol. Survey Canada Pap. 78-10, p. 283-314.
Morrison, M.A. (1978) The use of immobile elements to distinguish the paleotectonic affinities of metabasalts: application to Paleocene basalts of Mull and Skye, N.W. Scotland. Earth Planet. Sci. Lett., v. 39, p. 407-416.
Muecke, G.K., Pride, C., and Sarkar, P. (1979) Rare-earth element geochemistry of regional metamorphic rocks. In: Ahrens, L.H. (ed) Origin and distribution of the elements. Pergamon Press, Elmsford, N. Y., p. 449-464.
Pearce, J.A. (1982) Trace elements characteristics. In: Thorpe, R.S. (ed) Andesites: Orogenic andesites and related rocks. John Wiley & Sons, New York, p. 525-548.
Pearce, J.A. and Cann, J.R. (1973) Tectonic setting of basic volcanic rocksdetermining using trace element analyses. Earth Planet. Sci. Lett., v. 19, p. 290-300.
Pearce, J.A. and Norry, M.J. (1979) Petrogenetic implications of Ti, Sr, Y and Nb variations in volcanic rocks. Contrib. Mineral. Petrol., v. 69, p. 33-47.
Peccerillo, A. and Taylor, S.R. (1976) Geochemistry of Eocene calc-alkaline volcanic rocks from the Kastsmonu area, northern Turkey. Contrib. Mineral. Petrol., v. 58, p. 63-81.
Pharaoh, T.C. and Pearce, J.A. (1984) Geochemical evidence for the geotectonic setting of early Proterozoic metavolcanic sequences in Lapland. Precambrian Res., v. 25, p. 283-308.
Saunders, A.D., Tarney, J., Stern, C.R., and DeLziel, I.W.D. (1979) Geochemistry of Mesozoic marginal basin floor igneous rocks from southern Chile. Geol. Soc. Am. Bull., Part I, v. 90, p. 237-258.
Sims, P.K. (1976) Precambrian tectonics and mineral deposits, Lake Superior region. Econ. Geol., v. 71, p. 1092-1127.
Sims, P.K. (1988) Evolution of the early Proterozoic Wisconsin magmatic terrane of the Penokean Orogeny. (abstr.) 34th Annu. Inst. Lake Superior Geol., Marquette, Michigan, p. 100.
Sun, S.S. and Nesbitt, R.W. (1978) Geochemical regularities and genetic significance of ophiolitic basalts. Geol., v. 6, p. 689-693.
Thompson, R.N. (1982) Magmatism of the British Tertiary Volcanic Province. Scottish J. Geol., v. 18, Part I, p. 1-108.
Ueng, W.C., Fox, T.P., Larue, D.K., and Wilband, J.T. (1988) Geochemistry and petrogenesis of the early Proterozoic Hemlock volcanic rocks and the Kiernan sills, southern Lake Superior region. Canadian J. Earth Sci., v. 25, p. 528-546.
Van Schmus, W.R. (1976) Early and middle Proterozoic history of the Great Lake area, North America. Phil. Trans. Royal Soc. London, Series A, v. 280, p. 605-628.
Viereck, L.G., Flower, M.F.J., Hertogen, J., and Schmincke, H.U. (in press) The genesis and significance of N-MORBs. Contrib. Mineral. Petrol.
Watters, B.R. and Pearce, J.A. (1987) Metavolcanic rocks of the La Ronge Domain in the Churchill Province, Saskatatchewan: geochemical evidence for a volcanic arc origin. In: Pharaoh, T.C., Beckinsale, R.D., and Rickard, D. (eds) Geochemistry and mineralization of Proterozoic volcanic suites. Geol. Soc. Special Publication, no. 33, p. 167-182.
Weaver, S.D., Saunders, A.D., Pankhrust, R.J., and Tarney, J. (1979) A geochemical study of magmatism associated with the initial stages of back-arc spreading. Contrib. Mineral. Petrol., v. 68, p. 151-169.
Wood, D.A., Gibson, I.L., and Thompson, R.N. (1976) Elemental mobility during zeolite facies metamorphism of the Tertiary basalts of eastern Iceland. Contrib. Mineral. Petrol., v. 55, p. 241-254.

Manuscript received 19 September 1991.

북부 미시간 지역에 분포하는 선캠브리아기의 염기성 암맥에 대한 지화학적인 연구

위 수 민

요약: 본 논문은 슈피리어호 남부에 분포하는 선캠브리아기의 염기성 암맥들에 대하여 마그마의 기원과 그들이 생성될 당시의 지구조적인 환경을 알기 위하여 암석 및 지화학적인 연구가 행하여 졌다. 46개의 시료에 대한 주성분, 미량원소 및 희토류 원소들에 대한 화학분석이 이루어졌다. 이들의 화학성분은 전형적인 콘티넨탈 쏠레아이트 (contiental tholeiite)의 성격을 띄우며, 다소 철성분이 부화된 분화경향을 나타낸다. 부동원소 (immobile element)들을 이용한 tectonic discrimination diagram 에 의하면 모 마그마는 현재의 T-type MORB와 유사한 Ti의 함량이 많은 쏠레아이틱(tholeiitic)현무암으로 사료된다. 분화가 진행될수록 암석의 화학적 성질은 지각과의 동화작용(crustral asimilation)에 의해 많은 영향을 받은것으로 나타난다. 분화가 많이 진행된 암석들은 Rb, K, Ba, Th 과 같은

LIL원소의 증가를 보인 반면에 Nb, P, Ti과 같은 HFS 원소들은 그들과 물리, 화학적 성질이 비슷한 이웃한 원소들보다 현저한 감소를 나타내었다. 이러한 특징은 마그마의 기원에서 유래된것 뿐만 아니라 지각과의 동화작용이 병행함으로 기인되었다고 사료된다. 이 암석들의 지화학적 특성을 살펴보면 지각의 섭입과 관련되어(subduction related)생성된 암석의 화학성분과는 현저한 차이를 나타내며, 판(板)내에서 생성된 현무암(Within plate basalt)과 해양지각에서 형성된 현무암 (MORB)에서 보이는 특성을 나타낸다. 이러한 지화학적인 특성을 살펴볼때 이 암석들은 rifting과 같은 extensional tectonic 환경에서 생성된 것으로 사료된다.